

Effect of Nanosilica on The Formation of Calcium sulphoaluminate Hydrates Prepared from Nanomaterials

H. El-Didamony, B. A. Sabrah, S. Abd El-Aleem Mohamed, H. Gouda

Abstract- Nano-materials such as nanosilica (NS), nano-calcium hydroxide $\{Ca(OH)_2\}$, and nano-aluminum hydroxide $\{Al(OH)_3\}$ have been synthesized using a suitable method. In addition, gypsum has been prepared by precipitation method. The as prepared nano materials are characterized using x-ray diffraction (XRD), transmission electron microscopy. The average particle sizes are 15 nm, 49 nm and 25 for NS, $Ca(OH)_2$ and $Al(OH)_3$, respectively. These nano-materials are mixed with gypsum in a stoichiometric ratio to form ettringite as well as monosulphate mixes. NS was added to these mixes and hydrated at room temperature up to 28 days. All hydrated samples were characterized by performing chemical methods, XRD, differential thermal analysis, and thermal gravimetric analysis techniques. It was found that, the disappearance of $Ca(OH)_2$ due to its consumption during the reaction with NS stabilizes ettringite formation.

Keywords: Ettringite, ettringite+NS, hydration time, characterization techniques.

I. INTRODUCTION

Nano-particles (NPs) have attracted more attention and applied in many fields to fabricate new materials with novel functions, due to their unique physical, chemical and mechanical properties. Addition of NPs, even at a very small amount, to cement-based material enhances its workability, strength gain, and durability [1]. The role of NPs in cement can be summarized as follows: i) they act as fillers in the empty spaces as well as crystallization centers of hydrated products to increase cement hydration. ii) NPs assist towards the formation of small sized CH crystals and homogeneous clusters of C-S-H. iii) They improve the structure of interfacial transitional zone (ITZ) [2, 3]. During the last decade, different NPs have been used in concrete such as SiO_2 , $CaCO_3$, TiO_2 , ZnO_2 , Al_2O_3 , and Fe_2O_3 . Among of them, nano- SiO_2 (NS) has been extensively used in cementitious system [4–9]. This is mainly due to that, NS-particles enhance the compressive strength and reduces the permeability of hardened concrete because of its pozzolanic properties, which result in finer hydrated phases and densified microstructure (nano-filler and anti- $Ca(OH)_2$ -leaching effect) [10–13]. Ji [14] demonstrated that, nanosilica (NS) can react with lime and reduce its size as well as amount, thus decreasing ITZ between aggregates and therefore the cement paste becomes more dense.

Revised Version Manuscript Received on October 06, 2015.

H. El-Didamony, Department of Chemistry, Faculty of Science, Zagazig University, Zagazig, Egypt.

B. A. Sabrah, Department of Chemistry, Faculty of Science, Fayoum University, Fayoum, Egypt.

S. Abd El-Aleem Mohamed, Department of Chemistry, Faculty of Science, Fayoum University, Fayoum, Egypt.

H. Gouda, Department of Chemistry, Faculty of Science, Fayoum University, Fayoum, Egypt.

In addition, the NS-particles act as nuclei to fill the voids of the CSH structure and tightly bond with CSH particles. This means that, NS reduces the calcium leaching rate of cement pastes, and therefore increasing their durability [15, 16]. Ettringite, $Ca_6Al_2(OH)_{12}(SO_4)_3 \cdot 26H_2O$, is a naturally occurring mineral found in Germany for the first time [17]. This mineral is characterized by a high content of water. Molecules and is important for cement technology, because it appears as an early stage hydrated product of Portland cement (PC). Also, it has a wide application range to another types of cement called “regulated set cement” [18, 19] and “calciumsulphoaluminate cement” [20, 21], in which ettringite plays a crucial role on the early strength development of these novel cements. Another application is to grout in which quick setting of slurry is required [22]. Others are to paper coating commercially called “Santi White,” in which whiteness and impermeability are requested [23, 24].

Monosulfate ($3CaO \cdot Al_2O_3 \cdot CaSO_4 \cdot 12H_2O$) is related sulfoaluminate compound. In cement nomenclature, ettringite is also referred to as AFt and monosulfate as AFm. The formation of ettringite while the concrete is in a plastic state contributes the initial setting of concrete. Alternatively, ettringite formation after concrete has been set into a rigid, solid mass can be deleterious and can cause the loss of structural integrity. This dual character is due to the increase of solid specific volume accompanied with ettringite formation. In the literature, the expansion is attributed to ettringite formation with needle like structure [25]. AFm incorporates only 1 mole of sulfate and exhibits a plate like microstructural morphology [26]. The formation of monosulfate in hardened concrete is generally not considered deleterious, since its formation causes less expansion than does that of ettringite. There is, however, evidence in the literature which indicates that, monosulfate formation also causes expansion [27]. Ettringite can be synthesized by heating an aqueous suspension containing its constituent powders. There are two proposed methods for ettringite synthesis; One of them is the heating of suspension containing both calcium hydroxide (CH) and $Al_2(SO_4)_3$. The second includes heating of suspension containing CH, $Al(OH)_3$ in presence of gypsum (C_5H_2). Especially in the second case in which gypsum is used as a source of SO_4^{2-} instead of $Al_2(SO_4)_3$, the reaction becomes much difficult to proceed. Although ettringite can be partly formed by heating the mixture of $Ca(OH)_2$, $Al(OH)_3$ and gypsum. Most of gypsum still remains and an intermediate compound, i.e., monosulphate is formed. A novel technique is strongly required to synthesize ettringite monophase from these aqueous suspensions under atmospheric pressure [28]. In addition, Clark and Brown [29] reported on the formation of

the ettringite and monosulfate from tricalcium aluminate ($3\text{CaO}\cdot\text{Al}_2\text{O}_3$), gypsum ($\text{CaSO}_4\cdot 2\text{H}_2\text{O}$), and sodium hydroxide (NaOH) solutions. It was found that hydration in deionized water produced ettringite and monosulfate as the dominant crystalline phases, regardless of temperature. Thermal analysis and XRD data indicated that, U-phase formation becomes the dominant reaction with the increase of NaOH concentration. El Didamony et al. [30] synthesized $\text{C}_4\text{A}_3\text{S}$, monosulphate mix ($\text{C}_4\text{A}\text{S}$) and active $\beta\text{-C}_2\text{S}$ from nano-materials at $\sim 1250^\circ\text{C}$. The hydration mechanism was studied by XRD and DSC techniques as well as the determined from chemically combined water contents (Wn,%) of cement pastes with curing time. The results revealed that, the ettringite as hydration product is first formed in the monosulphate mix, which then converted into monosulphate hydrate. On the other side, the rate of hydration of active $\beta\text{-C}_2\text{S}$ increases linearly with hydration time from 3 up to 90 days, whereas, the traditional $\beta\text{-C}_2\text{S}$ hydration increases with lower rate up to 90 days, due to the thermodynamic stability of traditional belite structure. More interest, the formation of active belite and sulphoaluminate phases from nano-materials has lower energy requirements and lesser formation of $\text{Ca}(\text{OH})_2$ [31]. Since the ettringite is expansive in the presence of lime so that it has special applications such as shrinkage-resistant and self-stressing cements. On the other hand, the formed ettringite in the absence of lime is non-expansive and generates high early strength in cementitious system. This last property was exploited to develop a concrete with high early strength [32]. In this work, it was aimed to throw light on the effect of nanosilica on the ettringite as well as monosulphate mixes that prepared from nano-materials as an extension of our previous work [30]. Accordingly, the preparation of sulphoaluminate phases was carried out by using nano-materials. The prepared samples were characterized using X-ray diffraction (XRD), differential thermal analysis (DTA), and thermal gravimetric analysis (TGA) techniques.

II. Materials and Experimentals

II (A). Preparation of sulphoaluminate phases

The materials used in this work were nano- SiO_2 , nano- $\text{Al}(\text{OH})_3$, nano- $\text{Ca}(\text{OH})_2$, and gypsum. The nano- $\text{Al}(\text{OH})_3$ was prepared from Al-dross after leaching with HCl, then precipitated by ammonia solution at $\text{pH}=8$ [33]. NS was also synthesized by acidic hydrolysis of sodium silicate (Na_2SiO_3) using (0.5N) HCl and slowly stirred at 60°C at pH range 1-2 [34].

Nano CH was prepared by separately dissolving $\text{Ca}(\text{NO}_3)_2\cdot 4\text{H}_2\text{O}$ (0.5 M) and NaOH (0.7 N) in 50 mL distilled water (DW), then stirred for 10 min at room temperature. The prepared mix was irradiated by microwave energy using domestic microwave oven (frequency 2.45 GHz and maximum power 800 W) in ambient atmosphere for 10 min. After this, the solution was allowed to cool in air; the resulting precipitate was collected by vacuum filtration, washed with DW and absolute ethanol and dried in vacuum at 80°C for 1h [35]. C_5H_2 was prepared by precipitation method through the reaction between calcium acetate and ammonium sulphate.

The NPs were characterized using XRD and transmission electron microscopy (TEM), to be used for the preparation of sulphoaluminate phases (Ettringite and Monosulphate). The mix composition of Ettringite + NS and Monosulphate + NS mixtures has molar ratios of $3\text{CaO}\cdot\text{Al}_2\text{O}_3\cdot 3\text{CaSO}_4\cdot\text{NS}$ and $3\text{CaO}\cdot\text{Al}_2\text{O}_3\cdot\text{CaSO}_4\cdot\text{NS}$, respectively. The dry constituents for each mix composition were mechanically mixed in a ball mill for 30 min. to achieve complete homogeneity, and then hydrated for 28 days. The four mixtures (ettringite as well as ettringite + NS and monosulphate as well as monosulphate + NS) were mixed with the water of consistency according to ASTM designation C_{191} [36]. The hydration kinetics of the pastes was studied up to 28 d. At each testing time, the hydration was stopped as in previous works [37, 38]. Some selected samples were analyzed using XRD, DTA, and TGA techniques. Also, the combined water contents of the investigated samples were determined on the ignited weight basis after firing at 1000°C . Also, the free gypsum was determined as in a previous work [39].

II (B). Characterization of the starting materials

Figure 1 (a, b and c) shows TEM photographs of the prepared NS, nano- $\text{Al}(\text{OH})_3$ and nano- $\text{Ca}(\text{OH})_2$. It was revealed that, the particle size of NS, nano- $\text{Al}(\text{OH})_3$ and nano- $\text{Ca}(\text{OH})_2$ is about 15, 25 and 49 nm respectively. XRD patterns revealed that, NS and $\text{Al}(\text{OH})_3$ show amorphous structure. On the other hand, both C_5H_2 and CH have crystalline structure as shown in Fig.2 (b & d).

III. Results and Discussion

III (A). Effect of NS on the hydration of ettringite mix with curing time

X-ray diffraction analysis

Figure 5 (a-c) depicts the XRD patterns of the ettringite mix with curing time. It is obvious that the ettringite and gypsum are the major phases with the appearance of CH up to 28 d of hydration. The monosulphate phase has no reflection peaks within the accuracy of X-ray experiment [31]. The presence of gypsum up to 28 d is mainly due to the retardation of the hydration reaction by the formation of a coating layer of ettringite on the surface of the reactants. This retardation proceeds with the diffusion of SO_4^{2-} through the coating layer in the earlier stages forming more ettringite than that of latter hydration periods [40-44]. It can be concluded that the ettringite formation increases at early ages of hydration up to 3 d, whereas gypsum decreases with time, due to the partial consumption of free gypsum.

In addition, the decrease in the peak heights of ettringite phase at later ages may be related to the partial conversion of the formed crystalline ettringite into an amorphous phase. Also, the CH peaks are still present up to 28 days.

The XRD patterns of ettringite + NS as a function of hydration time is shown in Fig. 3 (a-c). The XRD patterns illustrate the presence of ettringite and gypsum in addition to Portlandite at all curing times. The Portlandite is completely consumed after 28 d. It is concluded that, NS reacts with CH to give CSH gel [14], which can not be detected by XRD technique. It is clear that, the intensity of ettringite peaks increases up to 2 d, and then decreases at 28 d. On the other

side, the peak height of gypsum decreases with hydration time. This may be due to the same reason as mentioned previously discussed. The CH peak intensities decrease with curing time, due to its consumption during the formation of CSH and ettringite.

Thermal Analysis

Figure 5 (a,b) represents the DTA and TGA thermograms of ettringite mix. As seen from the figure, there are three pronounced endothermic peaks that located at 102, 146, and 417°C for 6h of hydration. The first two endothermic peaks are mainly related to the dehydration of ettringite and gypsum, respectively. It is also clear that, the peak intensity of ettringite increases with the hydration time because of the formation of some amorphous ettringite (as indicated from the XRD patterns). On the other hand, the peaks intensity of gypsum peaks decreases. The results of DTA are in a good agreement with those of XRD. In addition, the third endothermic peak that located around 417°C, is related to the dehydroxylation of $\text{Ca}(\text{OH})_2$ and its intensity slightly decreases with hydration time, indicating its consumption, produces ettringite. There is another broad endothermic peak located nearly at 700°C after 28 d, due to the partial formation of crystalline CaCO_3 [45, 46]. One noticed that, each change in the TGA thermogram corresponding to the identified endothermic peaks in DTA data. The main weight loss of this system is occurred at lower temperatures up to 200°C, owing to the excessive formation of ettringite and residual gypsum as well as Portlandite. The TGA results are consistent with those of DTA.

DTA and TGA thermograms of ettringite and (ettringite + NS) mixes hydrated at 28 d are graphically displayed in Fig. 6 (a,b). The results show that, the first endothermic peak at 102°C for ettringite + NS mix is more pronounced than that of ettringite mix. Also, the endothermic peak intensity of gypsum becomes lower with time as previously seen in the XRD patterns. Adding NS to the ettringite mix, the CH endothermic peak disappears. This is mainly attributed to the pozzolanic reaction of NS with CH, forming CSH or C_2ASH_8 . In addition, the CSH peak is not observed in the ettringite + NS mix, because it overlaps with those of ettringite peaks. The increase of the first endotherm in the presence of NS can be ascribed to the formation of CSH, which located at the same temperature of ettringite. However, the endothermic peak of CH at 417°C is present in the ettringite mix without NS. The intensity of calcium carbonate peak that is observed around 647°C in the hydrated ettringite is higher than that in the hydrated ettringite + NS mix, due to the depletion of free CH that is easily carbonated. The results of DTA are consistent with those of TGA.

Combined water content

The variation of combined water contents (Wn, %) of ettringite as well as ettringite+NS mixes with hydration time are plotted in Fig. 7. The results indicated that the Wn, % increases gradually with time up to 28 days for the all hydrated samples. This behavior can be explained according to the rapid ettringite formation, which has high water content. The variation of the Wn, % is pronounced up to 48 h due to the formation of more amount of ettringite in

addition to the residual gypsum, which have a high Wn, %. It can be noted that, the Wn, % of ettringite mix is higher than that of ettringite + NS, especially at the first 24 h. This may be due to the high pozzolanic reactivity of NS with CH [14]. From 24 h up to 28 d of hydration, the Wn, % of ettringite mix becomes lower than that of ettringite + NS mix because the CSH formation is accompanied with the ettringite phase as well as the residual gypsum. As the hydration time proceeds, the CH decreases due to the consumption of CH in the formation of ettringite and CSH phases.

Free gypsum

The free gypsum contents of ettringite and ettringite+NS mixes are plotted as a function of hydration time in Fig. 8. It is noticed that, the free gypsum decreases sharply either for ettringite or ettringite+NS mixes up to 28 d due to the consumption of free gypsum through the hydration reaction, forming ettringite. The free gypsum of ettringite + NS mix is lower than that of pure ettringite at any hydration time. This is mainly attributed to the decrease of free gypsum content in the mix composition. On the other hand, the behavior of the free gypsum is nearly the same, but with different values up to 28 d probably, NS accelerates the ettringite formation in the two hydrated mixes.

III (B). The hydration of Monosulphate Mix in presence and absence of NS

X-ray diffraction analysis

Figure 9 shows the XRD patterns of the hydrated monosulphate mix. It is clear that, the ettringite is formed after 6h and its intensity slightly increased or still constant up to 28d, owing to the continuous hydration of the mix constituents, forming ettringite. The gypsum peak intensity decreases with time and completely disappeared after 2 d, due to its consumption during hydration reaction forming ettringite. Also, the intensity of the CH peak decreases with time as mentioned above. The CH is present up to 28 d in contrast with free gypsum, which depleted after 2 d since monosulphate mix exhibits a high CH content according to the molar ratio. It can be concluded that the monosulphate phase is not formed and the ettringite phase is mainly present in the monosulphate mix.

The X-ray diffraction patterns of the hydrated monosulphate + NS mix as a function of hydration time is depicted in Fig. 10. The results show the presence of ettringite phase and free gypsum as well as CH at 6 h. The intensity of ettringite peaks increases with curing time, while that of gypsum decreases. The peak of gypsum disappears completely after 6 h and this is not observed in the ettringite + NS mix because of the fast hydration of the mix constituents. The calcium hydroxide is also completely consumed during the first few 6h. This is essentially due to the pozzolanic reaction of NS with CH, forming CSH gel in addition to its reaction during the formation of ettringite phase.

Thermal Analysis

Figure 11 represents the DTA/TGA thermograms of monosulphate mix. The broad endothermal effect at 130°C is mainly caused by the presence of ettringite and the small

endothermal effect at 180°C due to the dehydration of the gypsum after 6 h. As the hydration proceeds, the ettringite peak intensity increases and that of gypsum decreases until completely disappears at 28 d. The TGA peaks corresponding to the different hydration products behave in the same manner of DTA peaks. The endothermic peak at 310°C after 6h may be ascribed to the dehydroxylation of $\text{Al}(\text{OH})_3$ [45,46]. The last thermal effect at 460°C is related to the dehydroxylation of $\text{Ca}(\text{OH})_2$, and its intensity slightly decreases with curing time, indicating its consumption, producing the hydrated sulphoaluminate phases, or some carbonation as seen from TGA curves. One noted that, the TGA loss increases with curing time, due to the increase of ettringite formation.

Figure 12 illustrates the DTA and TGA thermograms of the hydrated monosulphate and monosulphate+NS mixes at 28 days. The DTA results show the appearance of some endothermic peaks at 120, 460 and 650–700°C. The endothermic peak located at 120°C is principally due to the ettringite dehydration and calcium silicate hydrates; this endotherm appears with a higher intensity in monosulphate + NS mix, which form excessive amounts of hydrated products, as compared with the monosulphate mix. The endotherm located at about 460°C is related to the $\text{Ca}(\text{OH})_2$ dehydroxylation. It is clear that, such endothermic peak appears only in the monosulphate mix. The disappearance of CH in presence of NS stabilizes the ettringite formation.

Combined water content

The combined water contents (W_n , %) of monosulphate and monosulphate + NS mixes as a function of curing time are represented in Fig. 13. The results indicate that the W_n , % increases for the hydrated samples up to 28 d, due to the progress of hydration. The W_n , % of monosulphate mix are higher than those of ettringite mix as observed in Fig. 8. This is mainly due to the increase of CaO content in monosulphate mix than that of ettringite mix, leading to the formation of more CH content. By comparing the W_n , % contents of monosulphate mix with those of monosulphate + NS. It is noted that the W_n , % of monosulphate + NS mix is higher than that of monosulphate mix up to 15h. This can be explained according to higher reactivity of NS with CH leading to the formation of excessive CSH in addition to ettringite. On the other hand, the lower W_n , % of monosulphate + NS than that of monosulphate mix after the first 15 h is attributed to the increase of the pozzolanic activity of NS, leading to the formation of successive and additional amount of CSH. Since the formation of CSH is on the expense of ettringite phase, the W_n , % of monosulphate+NS becomes lower than that of monosulphate mix. At later ages of hydration (beginning from 28 d), the W_n , % of monosulphate + NS mix is mainly due to the formation of more hydrated products or the higher efficiency of NS to absorb water.

Free gypsum

The free gypsum contents of monosulphate and (monosulphate + NS) mixes at different hydration times are plotted in Fig. 14. Obviously, the free gypsum decreases gradually with hydration time because of the continuous hydration of mix constituents, consuming gypsum in the

formation of sulphoaluminate phases. In addition, its content is higher in monosulphate mix than that of monosulphate + NS mix at all curing ages. This is attributed to the presence of NS in the mix, which accelerates the hydration reaction. The reaction of NS with some of free CH decreases the coating effect of CH on the hydrated phases. Therefore, the free gypsum content of monosulphate + NS mix decreases sharply up to 48h, then slightly up to 28 d. On the other hand, the free gypsum content of monosulphate mix decreases linearly with the time up to 28 d. The consumption rate of gypsum is nearly the same with the time.

IV. Conclusions

Based on the XRD, DTA, TGA and chemical methods, the formation of ettringite phase is enhanced after 6 h and increased with hydration time. Four endothermic peaks were observed in DTA thermograms consistent with TGA results. It can be predicted that, the hydration of ettringite and ettringite + NS mixes gives ettringite phase that increases on the expense of free gypsum with curing time. Similarly, the hydration of monosulphate mix gives ettringite only at the time interval (6 h up to 28 d). Generally, monosulphate hydrate can't be formed in the ettringite, ettringite + NS, monosulphate and monosulphate + NS mixes. The disappearance of calcium hydroxide, due to its consumption during the reaction with NS, stabilizes ettringite formation.

REFERENCES

1. Hou P., Qian J., Cheng X., and Shah S. P., "Effects of the pozzolanic reactivity of nano-SiO₂ on cement-based Materials", *Cem. Concr. Compos.*; 55 (2015), pp. 250–258.
2. Sanchez F., and Sobolev K., "Nanotechnology in concrete—a review", *Cem. Concr. Res.*; 24 (2010), pp. 2060-2071.
3. Zyganitidis I., Stefanidou M., Kalfagiannis N., and Logothetidis S., "Nano-mechanical characterization of cement-based pastes enriched with SiO₂ nano-particles", *Mat. Sci. Eng. B*; 176 (9) (2011), pp. 1580–1584.
4. Singh L. P., Karade S. R., Bhattacharyya S. K., Yousuf M. M., and Ahalawat S., "Beneficial role of nano-silica in cement based materials—a review", *Cem. Concr. Res.*; 47 (2013), pp. 1069-1077.
5. Said A. M., Zeidan M. S., Bassuoni M. T., and Tian Y., "Properties of concrete incorporating nano-silica", *Cem. Concr. Res.*; 36 (2012), pp. 838–844.
6. Nazari A., and Riahi S., "The effects of SiO₂ nanoparticles on physical and mechanical properties of high strength compacting concrete", *Compos. Part B: Eng.*; 42 (2011), pp. 570–578.
7. Quercia G., and Brouwers H. J. H., "Application of nano-silica (NS) in concrete mixtures", In Gregor Fisher, Mette Geiker, Ole Heddal, Lisbeth Ottosen, Henrik Stang (Eds.), 8th fib International Ph.D. Symposium in Civil Engineering. Lyngby, June 20-23 (2010), Denmark, pp. 431-436.
8. Zhidan R., Wei S., Haijun X., and Guang J., "Effects of nano-SiO₂ particles on the mechanical and microstructural properties of ultra-high performance cementitious composites", *Cem. Concr. Compos.*, 56 (2015), pp. 25–31.
9. Said A. M., Zeidan M. S., Bassuoni M. T., and Tian Y., "Properties of concrete incorporating nano-silica", *Cem. Concr. Res.*; 36 (2012), pp. 838–844.
10. Gaitero J. J., Campillo I., and Guerrero A., "Reduction of the calcium leaching rate of cement paste by addition of silica nano particles", *Cem. Concr. Res.*; 38 (2008), pp. 1112-1118.
11. Berra M., Carassiti F., Mangialardi T., Paolini A. E., and Sebastiani M., "Effects of nanosilica addition on workability and compressive strength of Portland cement pastes", *Constr. Build. Mater.*; 35 (2012), pp. 666–675.
12. Stefanidou M., and Papayianni I. "Influence of nano-SiO₂ on the Portland cement pastes Composites", *Compos. Part B: Eng.*; 43 (2012), pp. 2706–2710.
13. Maheswaran S., Bhuvaneshwari B., Palani G. S., Nagesh R. I. and

Kalaiselvam S., "An overview on the influence of nano silica in concrete and a research initiative", Res. J. Recent. Sci.; 2 (2013), pp. 17-24.

14. Ji T., "Preliminary study on the water permeability and microstructure of concrete incorporating nano-SiO₂", Cem. Concr. Res.; 35 (2005), pp. 1943-1947.

15. Qing Y., Zenan Z., Deyu K., and Rongshen C. H., "Influence of nano-SiO₂ addition on properties of hardened cement paste as compared with silica fume", Constr. Build. Mater.; 21 (2007), pp. 539-545.

16. Gaitero J. J., Campillo I., and Guerrero A., "Reduction of the calcium leaching rate of cement paste by addition of silica nanoparticles", Cem. Concr. Res.; 38 (2008), pp. 1112-1118.

17. Deb S. K., Manghani M. H., Ross K., and et al., "Raman scattering and X-ray diffraction study of the thermal decomposition of an ettringite-group crystal", Phys. Chem. Miner.; 30 (1) (2003), pp. 31—38.

18. Yamaguchi G., Uchikawa H., Takagi S., and Tukiya K., "Calcium-fluoroaluminate and ferrite phases in regulated set cement", Cem. Sci. Concr. Technol.; 26 (1972), pp. 41-48.

19. Uchikawa H., and Matsuzaki Y., "Newly developed epoch-making super high early strength cement", Bull. Ceram. Soc. Jpn.; 7 (4) (1972), pp. 249—261.

20. Viswanathan V. N., Raina S. J., and Chatterjee A. K., "An exploratory investigation on porsal cement", World Cem. Technol.; 9 (1978), pp. 109-118.

21. Ikeda K., "Cements along the Join C₄A₃F̄—CS", Proc. 7th Int. Symp. Chem. Cement, Paris; 3 (1980), pp. III-31—2III-36.

22. Takehiro M., "Hydration and setting of Portland cement added with calcium aluminate-based seters", Doctoral Dissertation, Yamaguchi Univ.; (2000), pp. 90.

23. Moore A. E. and Taylor H. F. W., "Crystal structure of ettringite", Acta Crystallogr., Sect. B: Struct. Crystallogr. Cryst. Chem.; 26 (1970), pp. 386—393.

24. Yamada H., "Inorganic materials for paper making", Bull. Ceram. Soc. Jpn.; 12 (2) (1982), pp. 159—163.

25. Odler I. and Jawed I., "Expansive reactions in concrete"; pp. 221—47 in Materials Science of Concrete II. Edited by J. Skalny and S. Mindess. American Ceramic Society, Westerville, OH; 1991.

26. Taylor H. F. W., "Cement Chemistry"; Academic Press, New York; (1990), pp. 167.

27. Li G., Le Bescop P., and Moranville M., "Expansion mechanism associated with the secondary formation of the U-Phase in cement-based systems containing high amounts of Na₂SO₄", Cem. Concr. Res.; 26 (2) (1996), pp. 195—201.

28. Zhang Q., Saito F., "Sonochemical synthesis of ettringite from a powder mixture suspended in water", Powder Technology; 107 (2000), pp. 43-47.

29. Clark B. A., Brown P.W., "The formation of calcium sulfoaluminate hydrate compounds, Part II", Cem. Concr. Res.; 30 (2000), pp. 233—240.

30. EL-Didamony H., EL-Sokkari T. M., Khalil K. H. A., Heikal M. and Ahmed I. A., "Hydration mechanisms of calcium sulphoaluminate C₄A₃F̄, C₄A₃F̄ phase and active belite β-C₂S", Ceramics-Silikáty; 56 (4) (2012), pp. 389-395.

31. El-Didamony H., Sharara A. M., Helmy I. M. and Abd-El-Aleem S., "Hydration characteristics of β-C₂S in the presence of some accelerators", Cem. Concr. Res.; 26 (1996), pp. 1179-1187.

32. Abd El-Raouf F., Ph.D. Thesis, Faculty of Science, Zagazig University, Egypt (2008).

33. Mathew L., Narayankutty S. K., in: International conference on advance in polymer technology, India (2010) 279.

34. El-Didamony H., Khalil K. H. A., Ahmed I. A., Heikal M., Preparation of β-dicalcium silicate (β-C₂S) and calcium sulfoaluminate (C₃A₃C̄) phases using non-traditional nano-materials, Constr. Build. Mater.; 35 (2012), pp.77.

35. ROY A. and Bhattacharya J., "Microwave-assisted synthesis and characterization of CaO Nanoparticles", International Journal of Nanoscience; 10(3) (2011), pp. 413-418.

36. ASTM Designation C191: "Standard test method for normal consistency and setting time of Hydraulic Cement, Annual book of ASTM standard", 04.01, 2008.

37. El-Didamony H., Haggag M. Y., Abo-El-Enein S. A., "Studies on expansive cement: II. Hydration kinetics, surface properties and microstructure", Cem. Concr. Res.; 8 (1978), pp. 351 - 358

38. El-Didamony H., "Application of differential thermogravimetry to the hydration of expansive cement pastes", Thermochimca Acta; 35(1980), pp. 201-209.

39. Taha A. S., El-Didamony H., Abo- El-Enein S. A., and Amer H.A., "Physico-chemical properties of suspended cement pastes", zement-

Kalk-Gips; 34 (1981), pp. 315-317.

40. Khalil K. A. A. and El-Didamony H., "Study on the hydration products of the system CaO-Al₂O₃-SO₃-SiO₂ with varying CaO molar ratio", Thermochimca Acta; 40 (1980), pp. 337-347.

41. Serry A. S., Taha M. A., El-Hemaly S. A. S., and El-Didamony H., "Metakaolin- lime hydration products", Thermochimca Acta; 79 (1984), pp. 103-110.

42. Mehta P. k., "Effect of lime on the hydration of pastes containing gypsum and calcium aluminates", J. Am. Ceram. Soc.; 56 (1973), pp. 315-319.

43. Mosalamy F. H., El-Hemaly S. A. S., Abd-El- Wahed M. G. A., and El-Didamony H., "The hydration of C₃A in the presence of CaSO₄ and Ca(OH)₂", Arab gulf journal of scientific research; 3 (1) (1985), pp. 133-142.

44. Amin A. M., Sabrah B. A., and El-Didamony H., "Pozzolanic activity of amorphous silica", Silicates industries; 5-6 (1992), pp. 77-82.

45. Ramachandran V.S., Evaluation of concrete admixtures using differential thermal technique, ACI/RILEM – Symposium (1985) on "Technology of concrete when pozzolans, slags and chemical admixtures are used", pp. 35-55, Monterrey, Mexico (1985).

46. Ramachandran V.S., Paroli R.M., Beaudoin JJ and Deglado A.H., Handbook of thermal analysis of construction materials, Noyes Publications Norwich, New York, USA (2002).

Figures

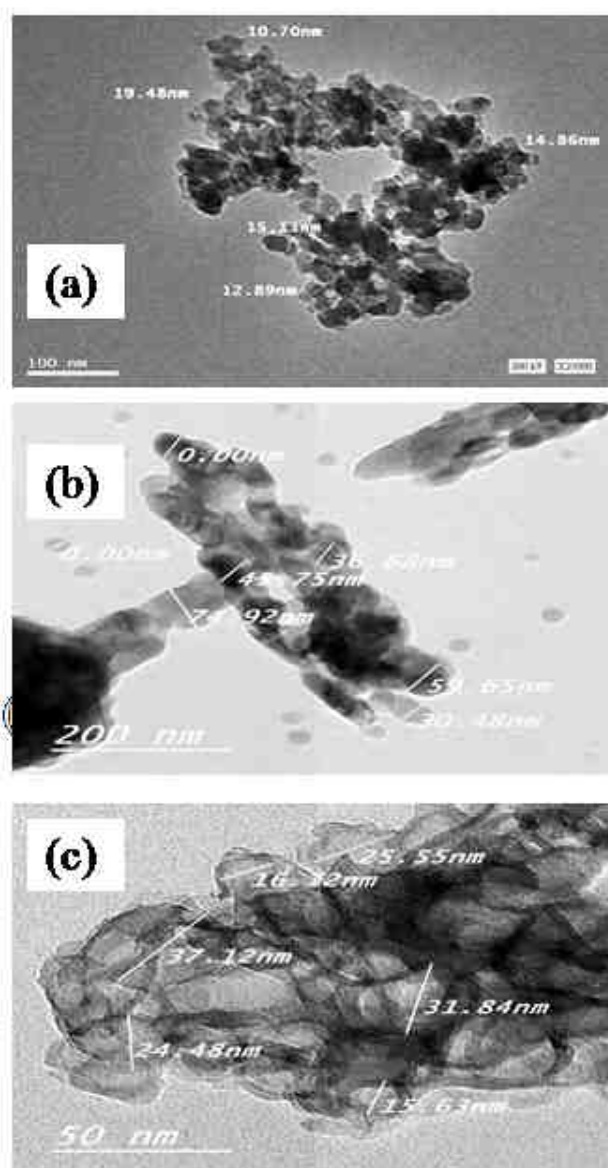


Fig. 1: Transmission electron micrographes (TEM) of: (a) nano-SiO₂, (b) nano- Ca(OH)₂ and (c) nano-

Al(OH)₃

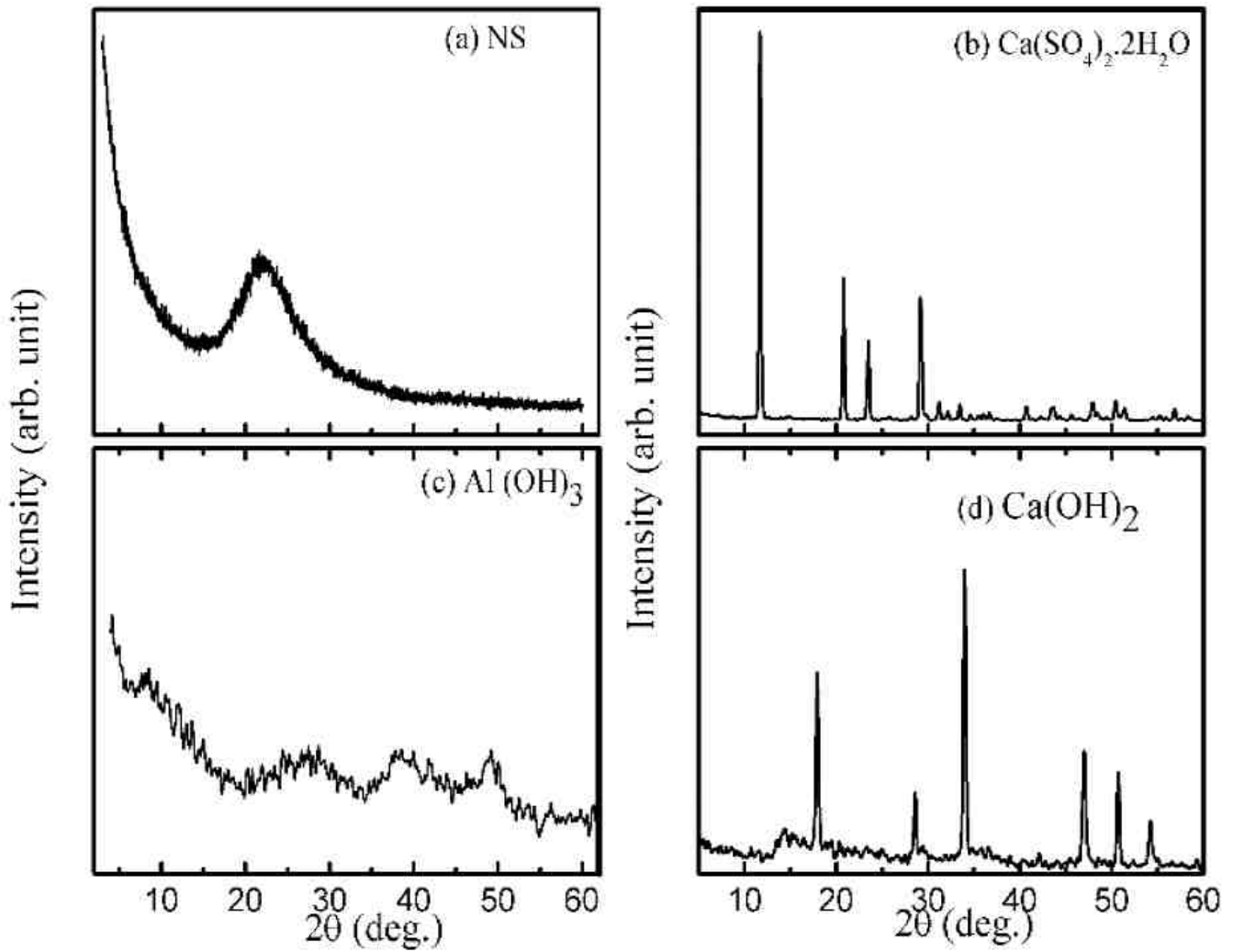


Fig. 2: XRD of: (a) NS, (b) Ca(SO₄)₂.2H₂O, (c) nano-Al(OH)₃ and (d) nano-Ca(OH)₂

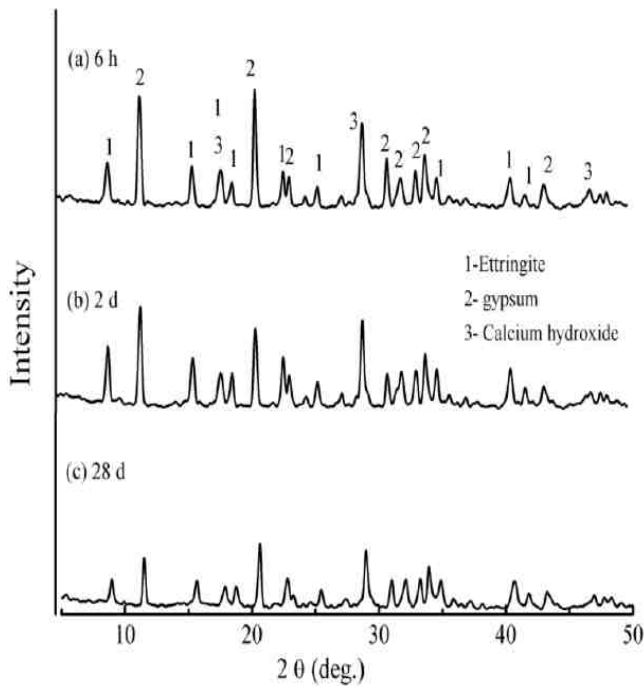


Fig. 3: XRD patterns of hydrated ettringite mix with curing times

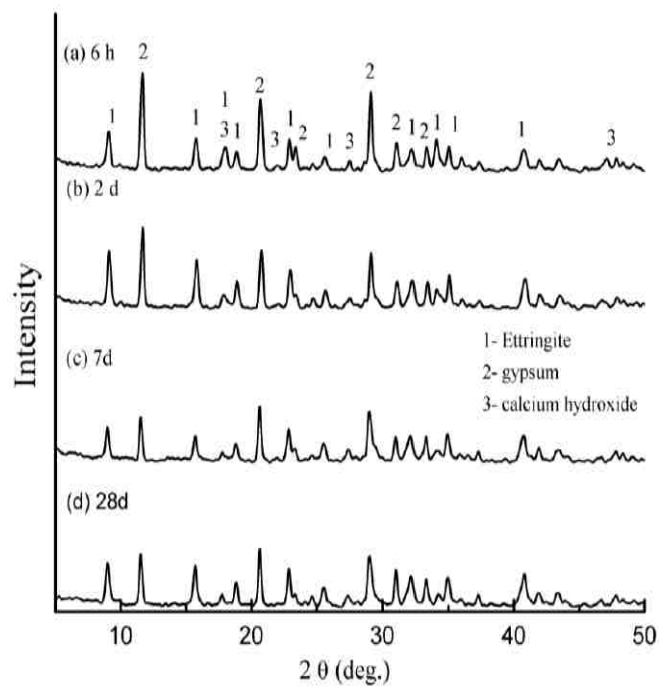


Fig. 4: XRD of hydrated ettringite + NS mix at different times

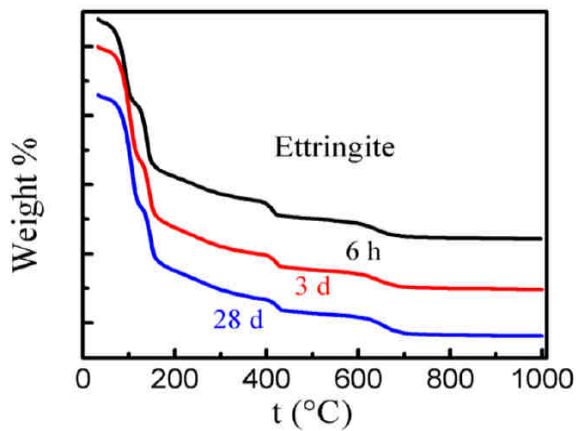
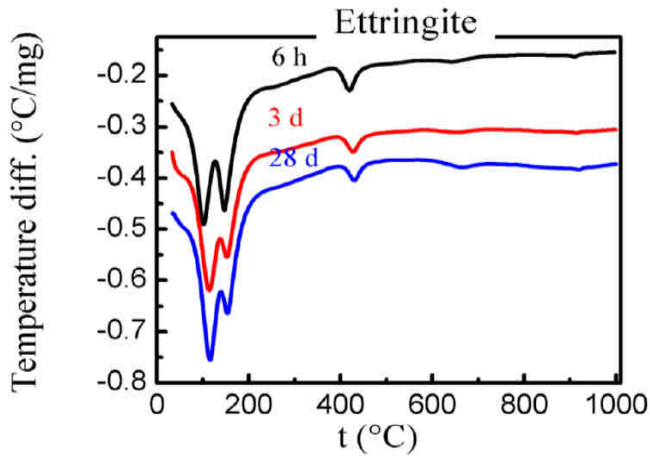


Fig. 5: DTA and TGA thermo grams of hydrated ettringite mix with curing time

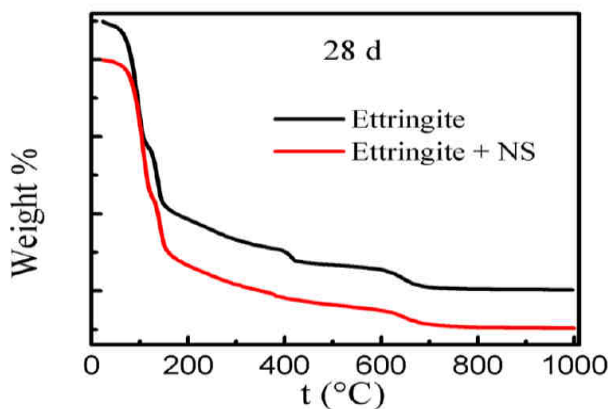
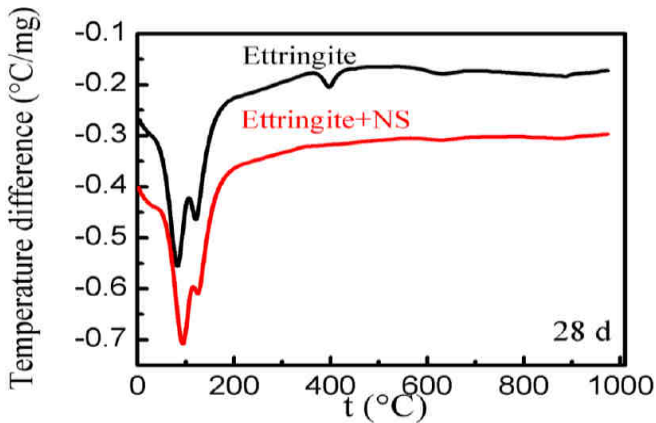


Fig. 6: DTA and TGA thermogram of ettringite and ettringite + NS mixes at 28 days

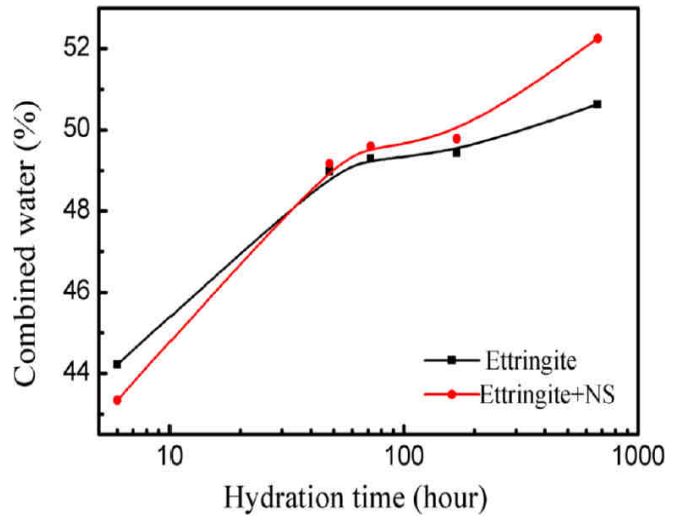


Fig. 7: Combined water contents of hydrated ettringite and ettringite + NS mixes at different times

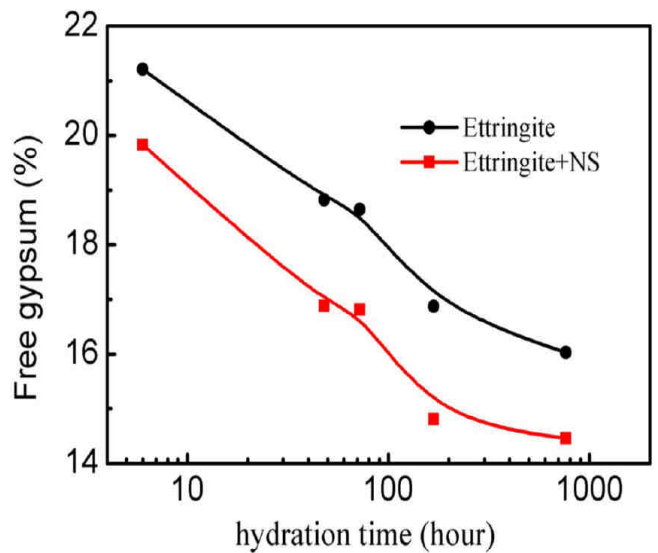


Fig. 8: Free gypsum contents of ettringite and ettringite + NS mixes with hydration time

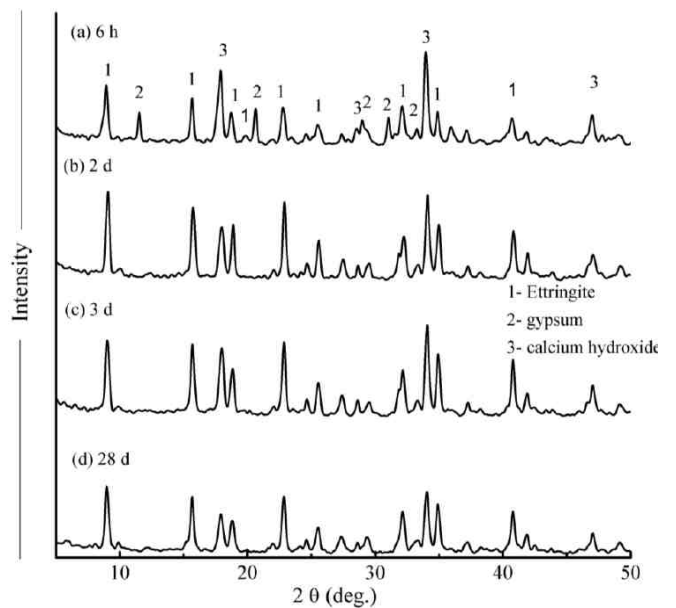


Fig. 9: XRD patterns of monosulphate mix at different hydration times

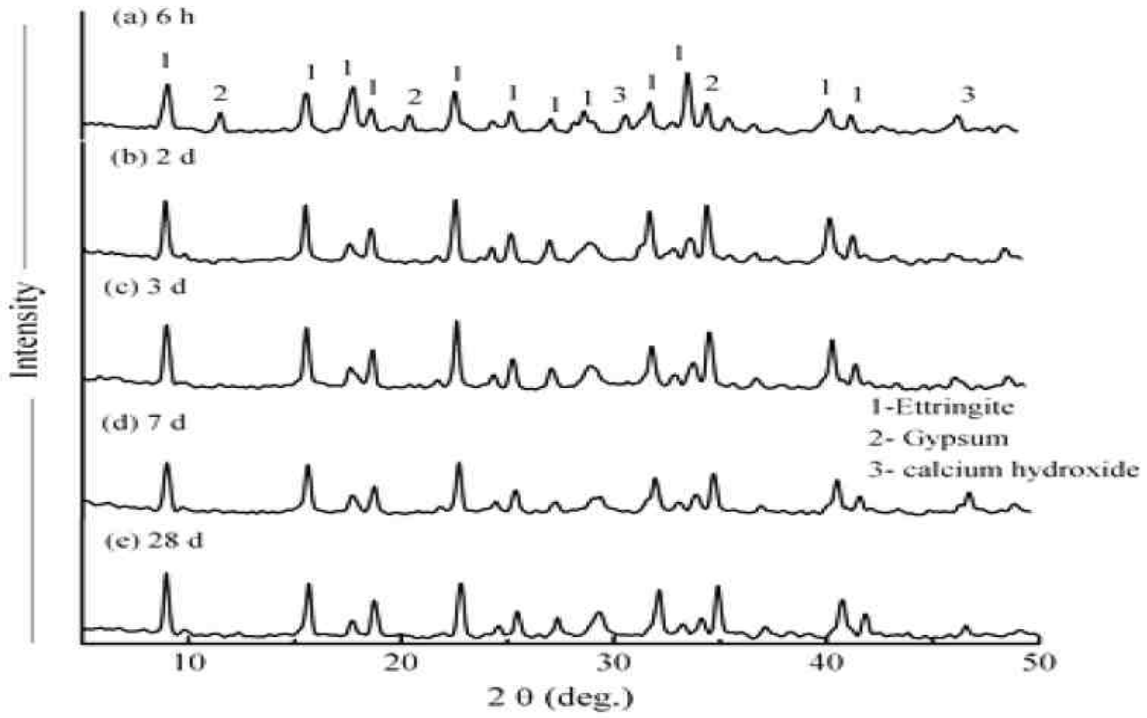


Fig. 10: XRD patterns of monosulphate + NS mix at different hydration times

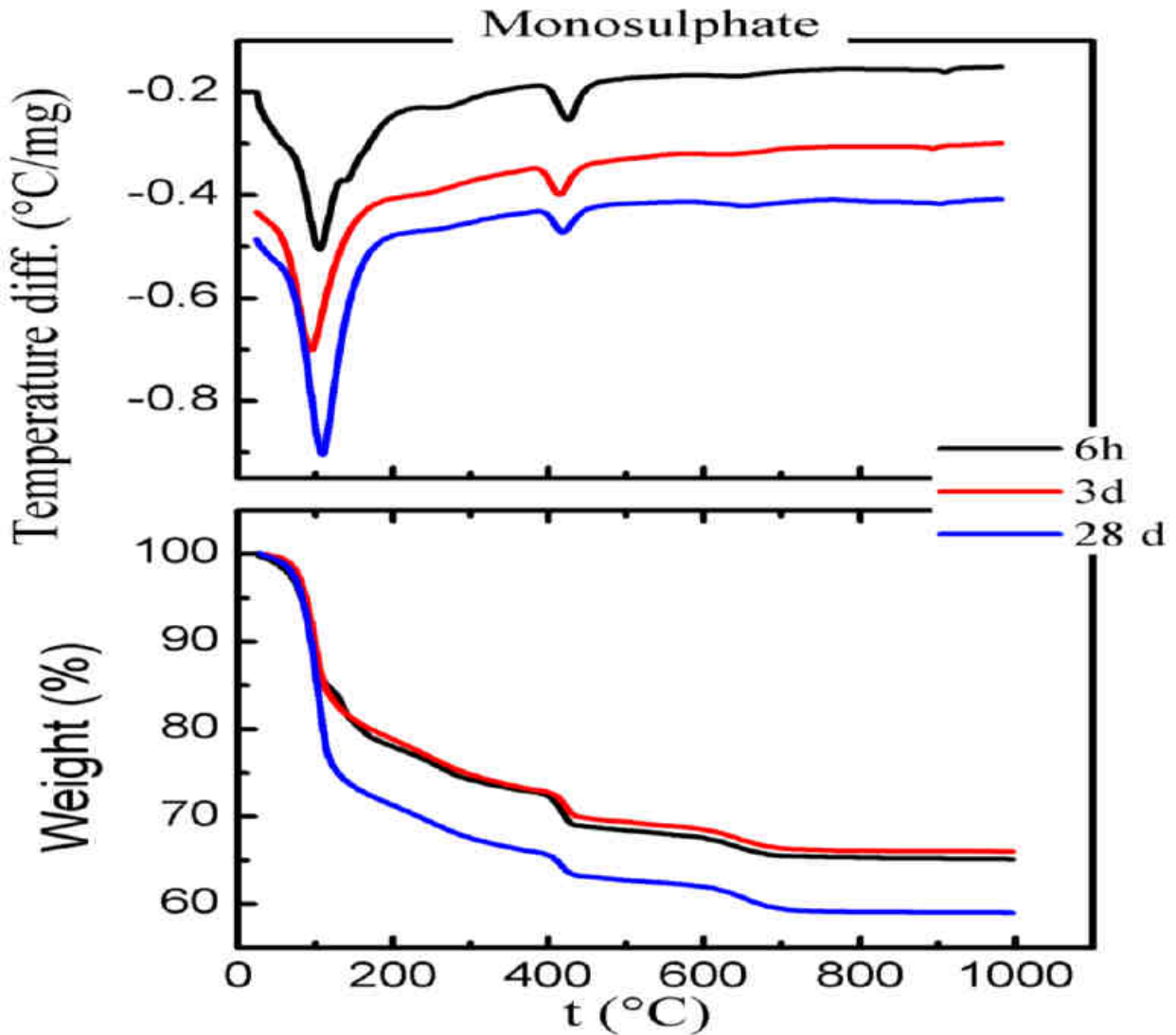


Fig. 11: DTA and TGA thermograms of hydrated monosulphate mix at different times

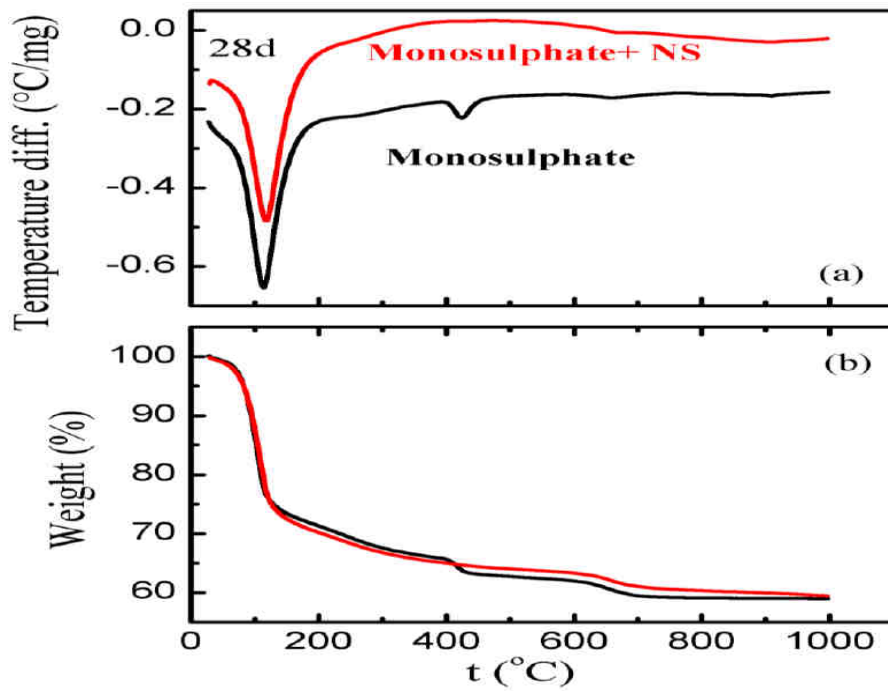


Fig. 12: DTA and TGA of monosulphate and monosulphate + NS mixes at 28 days

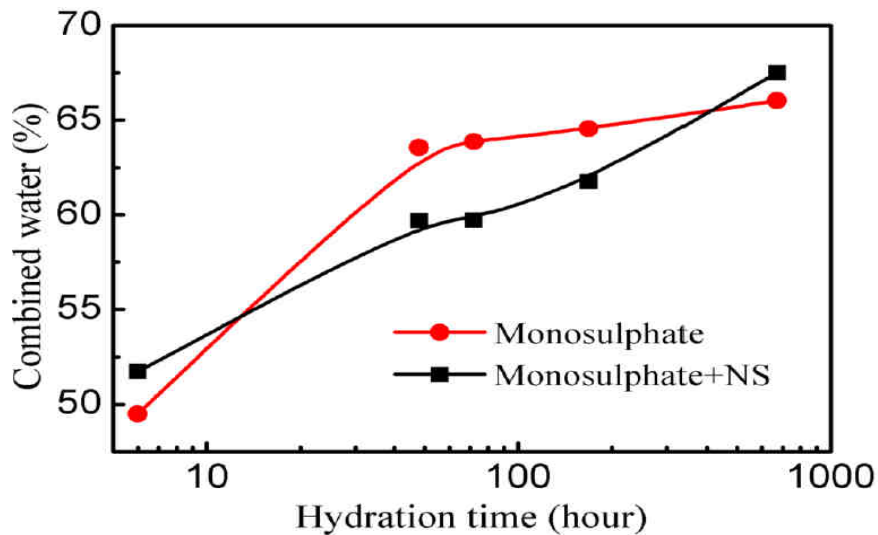


Fig. 13: Combined water contents of hydrated monosulphate and monosulphate + NS mixes at different times

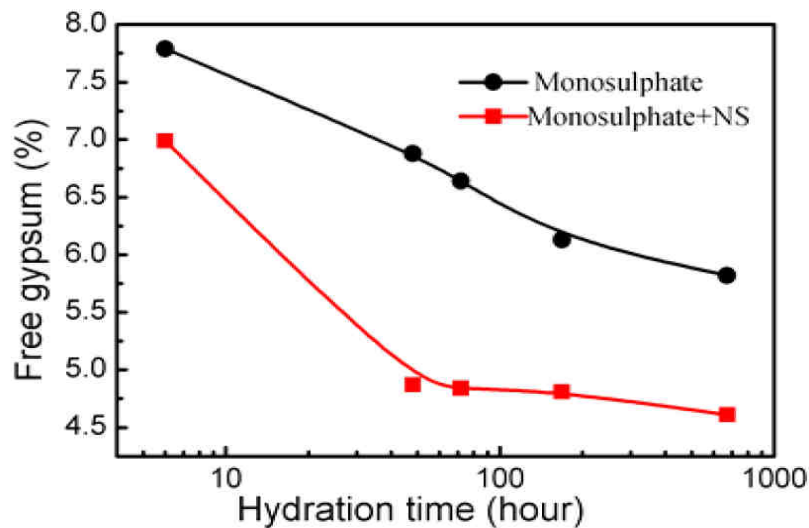


Fig. 14: The variation of free gypsum content of monosulphate and monosulphate +NS with hydration time